Coincidence of collective relaxation anomaly and specific heat peak in a bulk metallic glass-forming liquid

Abhishek Jaiswal, Andrey Podlesynak, Georg Ehlers, Rebecca Mills, Stephanie O'Keeffe, Joseph Stevick, James Kempton, Glenton Jelbert, Wojciech Dmowski, Konstantin Lokshin, Takeshi Egami, and Yang Zhang

Phys. Rev. B **92**, 024202 — Published 21 July 2015

DOI: 10.1103/PhysRevB.92.024202

Coincidence of collective relaxation anomaly and specific heat peak in a bulk metallic glass-forming liquid

Abhishek Jaiswal,[1] Andrey Podlesynak,[2] Georg Ehlers,[2] Rebecca Mills,[2] Stephanie O'Keeffe,[3] Joseph Stevick,[3] James Kempton,[3] Glenton Jelbert,[3] Wojciech Dmowski,[4] Konstantin Lokshin,[4] Takeshi Egami,[4] and Yang Zhang[1,5,*]

[1]*Department of Nuclear, Plasma and Radiological Engineering, University of Illinois at Urbana-Champaign, Urbana, IL 61801, USA*
[2]*Quantum Condensed Matter Division, Oak Ridge National Laboratory, Oak Ridge, TN 37831, USA*
[3]*Liquidmetal® Technologies, Rancho Santa Margarita, CA 92688, USA*
[4]*Department of Materials Science and Engineering, Department of Physics and Astronomy, University of Tennessee, Knoxville, TN 37996, USA*
[5]*Department of Materials Science and Engineering, University of Illinois at Urbana-Champaign, Urbana, Illinois 61801, USA*

(Dated: July 2, 2015)

The study of relaxational behavior of multi-component metallic liquids still holds the key to understanding and improving the glass-forming abilities of bulk metallic glasses. Herein, we report measurements of the collective relaxation times in a melted bulk metallic glass (LM601 $Zr_{51}Cu_{36}Ni_4Al_9$) in the kinetic regime (Q: 1.5 – 4.0 Å^{-1}) using Quasi-Elastic Neutron Scattering (QENS). The results reveal an unusual slope change in the Angell plots of the collective relaxation time of this metallic liquid around 950 °C, beyond the melting point of the material. Specific heat capacity measurement also reveals the presence of a peak around the same temperature. The coincidence is rationalized using Adams-Gibbs theory, and motivates more careful experimental and computational studies of the metallic liquids in the future.

PACS numbers: 64.70.pe, 61.05.F-, 61.20.Lc, 66.10.-x

I. INTRODUCTION

Bulk Metallic Glasses (BMGs) are attractive for engineering applications due to their remarkable mechanical properties, such as high tensile strength and hardness combined with their biocompatibility and magnetic properties[1–8]. Recent interests in Copper and Zirconium based glassy alloys are driven by their high glass-forming abilities[9–14]. Experimentally, the most common method to manufacture a metallic glass is by quenching the molten metallic liquid through the glass transition. By alloying multiple elements of various atomic sizes, crystallization can be suppressed, and consequently high quality metallic glasses with sizes as large as 5 to 10 cm can be produced[15,16].

Understanding the liquid state dynamics of such materials is essential to elucidate the physical properties of the glassy state[17–20]. Despite numerous active ongoing research efforts, a quantitative description of the glass transition of metallic liquids remains elusive. From a theoretical standpoint, there have been many developments in the past few decades. For example, the mode-coupling theory (MCT) of glass transition was proposed to describe the qualitative effects of mass transport in such dense liquids[21–24]. MCT predicts the existence of multiple relaxations in the collective atomic dynamics of such glass-forming liquids. Once the freezing of liquid-like motion results in structural arrest, mass transport occurs through hopping[25] in this frozen/glassy state. This microscopic dynamic singularity is manifested in the non-Arrhenius type behavior in fragile liquids. The timescale for such relaxations are in the range of 0.1 – 100 ps for various wavevector transfer Q in dense metallic melts and can be measured using the Quasi-Elastic Neutron Scattering (QENS)[26,27]. However, to what extent the theories based on idealized models can accurately describe the complex multi-component metallic liquids and their glass transitions remains an open question.

Various dynamical regimes can be identified in the wave-vector transfer Q space for liquid metals[28–30]. In the hydrodynamic limit ($Q \rightarrow 0$), dynamics is mainly governed by transport parameters (viscosity, self-diffusion coefficient, and thermal diffusivity). Following this, several authors have proposed a hypothetical isothermal regime (0.02 Å^{-1} < Q < 0.3 Å^{-1}) with negligible Q dependence of thermodynamic quantities, and electronic and ionic contributions to effective thermal diffusivity[30]. The generalized hydrodynamic regime above $Q \sim 0.3$ Å^{-1} is marked by frequency and wave-vector dependence of transport properties[31]. The kinetic regime occurs around the peak of $S(Q)$ and extends to a few subsequent oscillations. In this regime, Enskog's kinetic theory predicts dominant effect of an extended heat mode using hard sphere type framework in simple liquids[30]. At very large Q values, scattering experiments probe ballistic motions of particles with the distinct part of van Hove correlation function equaling zero.

There have been several studies regarding the mean self-dynamics of Cu-Zr based glass-forming liquids using QENS[19,26,27,32,33]. The relaxation behaviors of such

* To whom correspondence should be addressed. E-mail: zhyang@illinois.edu

melted liquid at small $Q < 1.5$ Å^{-1} have been studied. Fast β-relaxations characterizing rattling of atoms in cages formed by their neighbors and the subsequent α-relaxation responsible for viscous flow/diffusion has been characterized. Subsequently, the diffusive behavior or self-motions has been measured fors such liquids. In this paper, we present measurements of collective dynamics in the liquid state of an excellent bulk-glass former LM601 with the composition ($Zr_{51}Cu_{36}Ni_4Al_9$). The wave-vector transfer range presented in this paper is 1.5 – 4 Å^{-1}, which covers the first peak in the static structure factor of this material. The measured scattering spectrum is fitted with two models including a phenomenological and a theoretical treatment, and their temperature dependencies are presented. The atomic dynamics relevant in this Q-range quantifies the fast collective relaxations in the system.

II. METHODS

High quality lab-grade BMG samples of LM601 with atomic compositions $Zr_{51}Cu_{36}Ni_4Al_9$ were produced by Liquidmetal® Technologies Inc. using counter gravity cast. The samples were cast in slabs with dimensions of 40 mm × 30 mm × 5 mm and mass of ∼50 g. The heat capacity measurement was performed using a Netzsch Differential Scanning Calorimetry (DSC) 404c instrument in a high-purity inert argon atmosphere. A small piece of sample with a mass of ∼79 mg was used in a pyrolytic graphite crucible. The scanning rate was 20 K/min. Thermo-Gravimetric Analysis (TGA) and DSC measurements were also carried out using a Netzsch STA 449F1 in a high-vacuum and high-purity inert helium atmosphere. A small piece of sample with mass of 24 mg was used in an alumina crucible. TGA measurement confirmed that the sample mass remained unchanged during the temperature cycling.

Quasi-elastic neutron scattering measurements were carried out at the Cold Neutron Chopper Spectrometer (CNCS; Beam Line 5) at the Spallation Neutron Source (SNS) located at Oak Ridge National Laboratory (ORNL). An incident neutron beam of 12.07 meV in energy was used in the High Flux operational mode of the choppers. The energy resolution of the instrument (FWHM) in these operational conditions was ∼ 0.65 meV, and the wave vector transfer Q range was 0.5 – 4.3 Å^{-1}. LM601 samples were cut into rectangular sticks (1.5 mm × 30 mm × 1.5 mm) and stacked inside a cylindrical MgO crucible with a cylindrical MgO insert. The thickness of the sample is controlled as 1.75 mm (×2 layers) in order to avoid multiple scattering. The crucible was suspended to the thermocouples using thin platinum wires inside a high temperature furnace. A high-purity inert helium atmosphere in high vacuum (∼ 10^{-5} torr) was maintained during measurements. Two thermocouples were used at various locations to verify the uniformity of temperature inside the furnace. Samples were heated at a constant rate of 50 °C per hour during heating. Measurements at a specific temperature were carried out for approximately 5 hours to obtain good counting statistics. At 1100 °C, we were only able to perform 2-hour measurements due to beam-time constraint. We didn't measure even higher temperatures due to concerns about sample evaporation and beam-time constraint.

The total scattered neutron intensity spectrum was corrected for the time-independent background and normalized by white-beam vanadium run using the data reduction package *MantidPlot*[34]. The reduced data were then further interpolated to constant Q values using *MSlice* in *DAVE*[35]. Empty crucible was measured at room temperature and used for background subtraction. At high temperatures, the detailed balance factor is insignificant in the measured dynamic range and hence was ignored in further data analysis. The energy transfer range at the energy loss side is limited by the incident neutron energy and hence is much shorter than the energy gain side. Additional scattering from the instrument rendered a peak at ∼2.5 meV in the energy loss spectrum and couldn't be fully subtracted. Hence data analysis was performed on the energy gain spectrum that has much wider dynamic range. The MgO empty crucible measured at room temperature was used as the instrument energy resolution function. For the data fitting in the energy domain, the elastic peak of resolution function was represented by a sum of two Gaussian functions. The spectral shape of $S(Q, E)$ was fitted using Fourier Transform of the Kohlraush-William-Watts (KWW) stretched exponential function convoluted with the energy resolution function. Fittings in time domain were performed using Mode Coupling Theory (MCT) β-scaling framework. Structure factor $S(Q)$ of the sample were obtained by integrating the elastic scattering intensity in the energy range of $[-0.5, 0.5]$ meV.

III. RESULTS

Figure 1 shows the heat capacity c_p of the BMG sample LM601 obtained by the DSC measurement at a heating rate of 20 K/min. Glass transition in the sample sets in at 697 K and extends to roughly 730 K, marked by an endothermic shoulder. Immediately after that, the sample crystalizes at 773 K, marked by a significant exothermic peak. The crystallized state extends to 1170 K where it is completely melted, evidenced by a series of endothermic peaks in this mid-temperature range. A subsequent broad heat capacity peak is observed in the temperature range of 1250 – 1450 K, beyond the melting temperature of the sample. The inset magnified to the suitable temperature range clearly illustrates this heat capacity peak. A similar observation of an additional heat capacity peak above the liquidus temperature has been reported in Vit. 1 BMG[19]. Due to similarities in the composition of both systems, this heat capacity peak may turn out to be a key feature of Cu-Zr-Al based metallic

liquids.

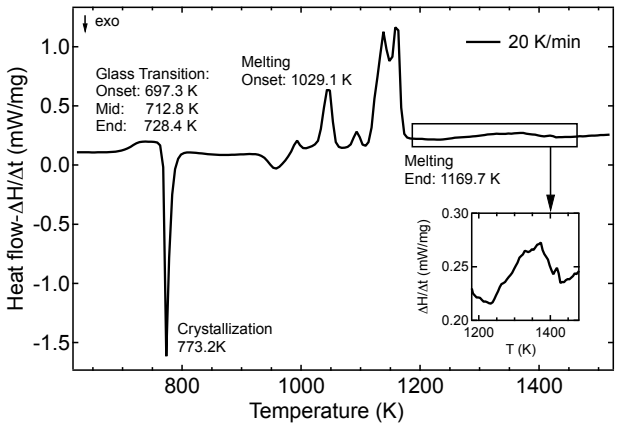

FIG. 1. Specific heat flow of BMG LM601 during a heating cycle of 20 K/min. Multiple phase transitions can be seen as the temperature is raised. Note that there is a broad yet well-defined heat capacity peak from 1250 to 1450 K, which is beyond the melting endpoint of the system. Inset shows the magnification of c_p peak in this temperature range.

In contrast to many similar QENS measurements[19,26,27,32,33] that are collected at Q values much lower than the structure factor $S(Q)$ peak, the contribution to the neutron scattering signal in the wave vector transfer Q range we measured predominantly comes from the coherent scattering of individual elements. The structure factor $S(Q)$ obtained by integrating the elastic scattering intensity in the energy transfer range of $[-0.5, 0.5]$ meV shows a series of transitions from glassy state to "supercooled liquid", to crystal, and to liquid state over a temperature range from 27 °C to 1050 °C (see Fig. 2). The elastic scattering data obtained using an elastic neutron scattering instrument doesn't provide as excellent Q-resolution and statistics as in a dedicated diffraction instrument. However, the quick examination of the evolution of the structure factor is useful to confirm the states of the sample, which agrees with the DSC curve. The positive and negative peaks near 1.8, 3.0, and 3.8 Å^{-1} in the temperature range between 900 °C and 1050 °C arises from the imperfect subtraction of the MgO sample container. The empty MgO container was only measured at room temperature due to beam-time constraint. The MgO Bragg peaks shift to higher Q values at higher temperatures because of thermal expansion, therefore, it is not possible to fully subtract this feature unless background measurements of empty MgO are also performed at the same exact configuration and temperature conditions. However, the contribution from the crucible scattering to the signal is predominantly in the elastic peak region and does not contribute to the quasi-elastic broadening. To ensure complete melting of the sample, we performed measurements at 900 °C for twice as long as we did for other temperatures.

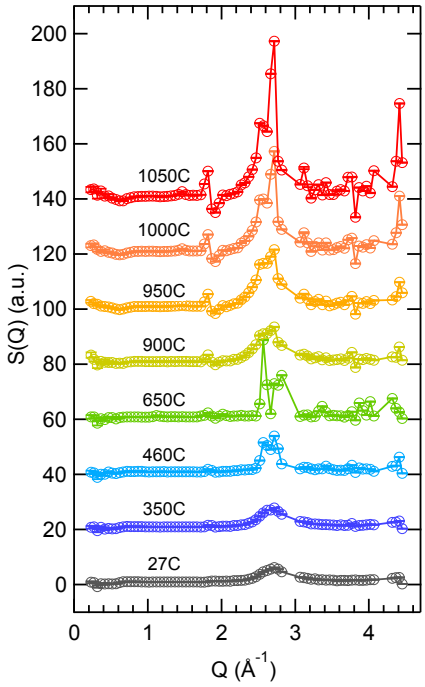

FIG. 2. Evolution of the structure factor $S(Q)$ of BMG LM601 at various temperatures, obtained by integrating the elastic scattering intensity at CNCS. As the temperature is raised, a series of transitions from glass to "supercooled liquid", to crystal, and finally to liquid state are clearly observed, in agreement with the DSC scan. The baselines have been shifted for each temperature for clarity. The positive and negative peaks near 1.8, 3, 3.8 Å^{-1} are due to the imperfect subtraction of the empty MgO crucible scattering, which is measured at room temperature only.

In the ensuing sections, we present analysis of QENS data using two common models for the relaxational behavior of liquids. The KWW model is applied to fit the data in energy domain, and the MCT β-scaling analysis is applied in the time domain. Using both methods, we intend to illustrate the model-independent nature of the results. The extracted relaxation times using both models exhibits a consistent temperature dependence, but differs slightly in value.

A. Phenomenological KWW analysis

The microscopic relaxation time of such metallic glass forming liquids is commonly quantified by applying the phenomenological stretched exponential KWW fitting to the measured Quasi-Elastic Neutron Scattering (QENS) spectrum in the energy domain. Figure 3 shows the measured dynamic structure factor of the sample at temperatures from 900 °C to 1100 °C around the structure factor peak of sample. The spectrum shows broadening at higher temperatures and a reduction in elastic scattering

intensity due to increasing atomic mobility in the liquid. In this Q-range, transport properties are dependent on the frequency and the wave-vector transfer[30]. Hence, the spectral shape of $S(Q,E)$ cannot be described by a single Lorentzian function. In this section, we show the results obtained by fitting the QENS spectra with a single KWW model. With one KWW relaxation model, the fit (Fig. 3) is reasonable below 3.5 Å^{-1}.

$$S(Q,E) = N\mathcal{F}\{F(Q,t)\} \otimes R(Q,E) + \text{Bkg} \qquad (1)$$

where N is the normalization factor; $F(Q,t)$ is the intermediate scattering function; $R(Q,E)$ is the Q-dependent instrument resolution function quantified as room temperature measurements of the empty crucible and Bkg accounts for the very fast motions. The intermediate scattering function is modeled as following KWW stretched exponential function:

$$F(Q,t) = A_Q \exp(-(t/\tau)^{\beta}). \qquad (2)$$

In the above equation, β is the stretching exponent, τ is the relaxation time, and A_Q is the effective Debye-Waller factor in a liquid. Due to the nature of fitting in Eq. (1), it is not possible to isolate A_Q as it is incorporated into N. Thus, the model depends on two essential fitting parameters: relaxation time τ and stretching exponent β.

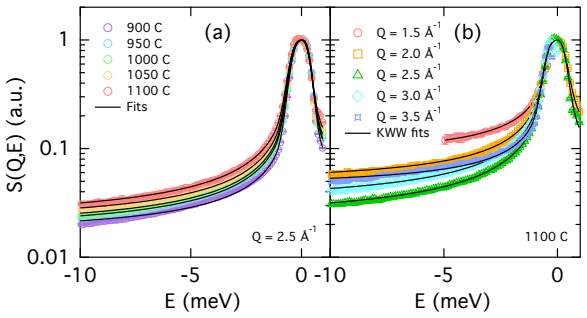

FIG. 3. (a) Quasi-Elastic Neutron Scattering (QENS) spectra of melted BMG LM601 at the vicinity of structure factor maximum. Solid lines denote the fit using Fourier transform of one Kohlrausch-Williams-Watts (KWW) stretched exponential function. (b) Q-dependence of measured spectra with KWW fittings at $T = 1100$ °C.

The extracted relaxation time using a single KWW model reveals an unusual temperature dependence characterized by a clear change of slope. Even more striking is the fact that τ at 950 °C and 1000 °C overlap at most Q values. Furthermore, the timescale of this relaxation lies in the range of 0.1 – 1.5 ps (Fig. 4) suggestive of fast β-relaxation in the system. The stretching exponent β is very small ($\sim 0.1 - 0.3$) indicating the highly stretched nature of this fast relaxation. β indicates the deviations from Debye exponential relaxation in the liquid. Such non-exponential behavior can arise from heterogeneous states in a liquid that relax exponentially, or from the atoms in the liquid that relax in an intrinsically nonexponential way thus causing a rise in cooperativity in the system[36]. In many metallic glass-forming liquid systems β is found to vary from 0.5 – 1.0 for self correlation functions[27,37,38]. Our fitting results show distinct results for β of collective correlation functions at all Q-values. Such a highly stretched nature of slow relaxations is a surprising revelation from the fittings. In the KWW model, τ and β are coupled. Hence to extract these two parameters unambiguously requires excellent data quality and wide dynamic range. To add to this complexity, energy resolution of the instrument progressively deteriorates away from the elastic peak. Usually, the beta relaxation process happens at a timescale of cage vibrations in the systems. In such multi-component liquids there is a distinct possibility of deviations from exponential behavior due to influences from local bond formation/breaking events at this Q-scale and the chemical disorder. Other fitting parameters do not show strong temperature dependence and are approximately constant in this range. The slope of the Angell plot is proportional to the activation energy of the material. A zero slope between 950 and 1000 °C implies an unrealistic zero activation energy. This is characteristic of some form of microscopic instability in the system. One of the connotations of such an instability is a phase transition within the liquid. As this temperature is sufficiently higher than the melting temperature of the sample, presence of crystalline phases cannot be regarded as an explanation for this instability.

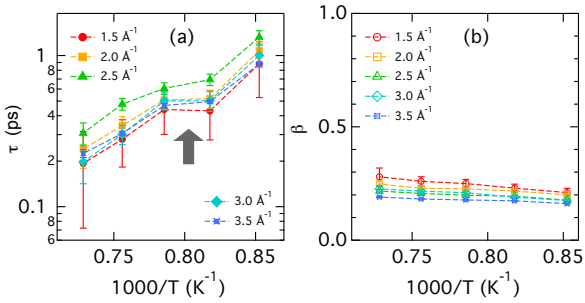

FIG. 4. (a) Relaxation time extracted from KWW fits of QENS data shows an interesting dip between 950 °C and 1000 °C. (b) Stretched exponent β_Q is very small and increases slightly with increasing temperature.

B. MCT β-scaling analysis

Mode coupling theory (MCT) provides a rigorous framework for analysis of QENS data, as it provides an analytical form of the intermediate scattering function $F(Q,t)$. By construction, the static quantities such as density, structure factor, etc. predict the dynamics in MCT. Thus, with increasing coupling the dynamics is slowed down and ultimately results in a structural arrest at a critical temperature T_c below which transport can

only happen through activated processes such as hopping. Although the idealized MCT predicted structural arrest does not occur in real systems, this framework still has important merits and has been utilized in analyzing metallic liquids above melting temperature with reasonable success[25–27,37,39]. Because of the large dynamic range in our QENS data, the timescale of measured dynamics involves fast β-relaxations. MCT provides an asymptotic form of the density correlation function for β-relaxation given as follows[40]:

$$F(Q,t) = f_Q + h_Q\ g_\lambda(t/t_\sigma), \tag{3}$$

where f_Q is the non-ergodicity parameter; h_Q is a scaling amplitude of β-relaxations; t_σ is the timescale of β-relaxation; and the time-dependent term $g_\lambda(t/t_\sigma)$ is determined completely by an exponent parameter λ. In theory, λ can be expressed in complex mathematical formulations in terms of structure factor for simple systems. In our analysis, following other works[26,39], we used a value of $\lambda = 0.77$, which is close to the value for hard-sphere mixtures[41], and is fixed throughout the temperature and Q values. In several relevant Cu-Zr based systems, the incoherent density correlator was fitted with a λ value of 0.77[26,27]. As the shape of β relaxation quantified by $g(t)$ is the same for both self and collective dynamics, use of this value in our analysis is justified[42]. The experimental data is inverse Fourier-transformed and deconvoluted with the resolution in time domain. In doing so, decay of $F(Q,t)$ at long times are affected and unreliable due to the small values of the resolution function.

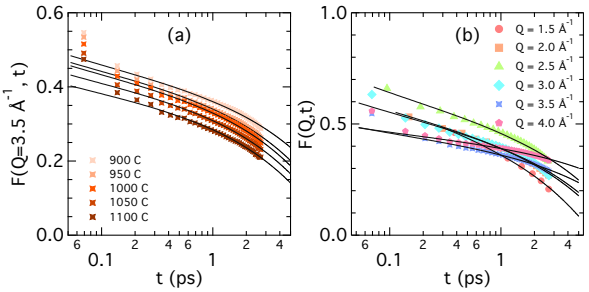

FIG. 5. (a) Temperature dependence of density correlation function $F(Q = 3.5\text{Å}^{-1}, t)$ for the melted $Zr_{51}Cu_{36}Ni_4Al_9$. (b) Wavevector transfer Q-dependence of $F(Q,t)$ at 900 °C shows that the relaxations shape $S(Q)$. The time range of $F(Q,t)$ shown characterizes the β-relaxation in this metallic melt. Solid lines denote the MCT β-scaling fits applied to the deconvolved density correlation function. At very short times, fast motions such as phonon contributions give rise to deviations from the fit.

The extracted β-relaxation time t_σ is consistent with results from KWW analysis in the preceding section. This Q–dependent relaxation time t_σ follows the shape of $S(Q)$, indicative of collective relaxation. Such a variation of t_σ in phase with $S(Q)$ is commonly known as the *de Gennes narrowing* and has been observed in several glass-formers[42–45]. The proximity of the observed relaxation decay at 950 °C and 1000 °C in Fig. 5 translates to a flattening of t_σ in Arrhenius plots, and a clear change in slope (Fig. 6). Such behavior is observed across all the Q values outlining the first $S(Q)$ peak in this melt. The interesting coincidence of the change in slope with the observed peak in the specific heat measurements (Fig. 1) suggests a thermodynamic origin of the dynamical features observed in relaxation time and is discussed in the ensuing section. The other fitting parameter f_Q reflects the shape of $S(Q)$ and shows weak temperature dependence; while h_Q shows the reverse $S(Q)$ shape dependence and also weak temperature dependence.

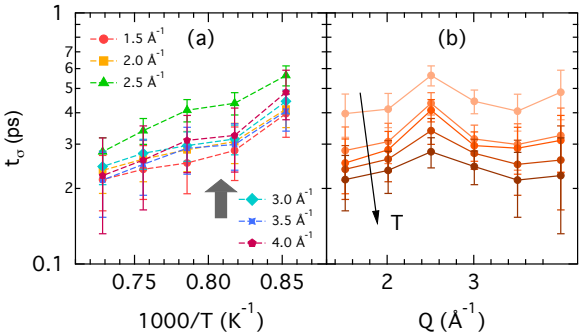

FIG. 6. (a) Arrhenius plots of t_σ at all Q values outlining the first peak in $S(Q)$. The extracted values range for 0.2 – 1 ps across the Q-range. An interesting dip in the relaxation time is observed between 950 °C and 1000 °C. (b) Q-dependence of t_σ clearly illustrates the de Gennes narrowing, signaling the collective nature of relaxation in the quaternary melt.

IV. DISCUSSIONS

The coincidence of the specific heat peak and the unusual change of slope of the relaxation time in the Angell plot could be understood from the Adam-Gibbs theory[46,47]. Adam-Gibbs theory provides a framework for connections between the transport coefficients and the configurational entropy S_{conf}. Our measurements quantify fast motions and as such cannot be directly applied with Adam-Gibbs theory. Nevertheless, we would apply it in the ensuing discussions to motivate a thermodynamic origin of our observations.

$$\tau = \tau_0 \exp\left(\frac{C}{TS_{conf}}\right), \tag{4}$$

τ_o is a prefactor with weak temperature dependence and C is a constant proportional to the free activation energy of co-operatively rearranging region. At such high temperatures, if we ignore the contributions of vibrations to entropy S and approximate the total entropy by the configurational part only, such that $S_{conf} \approx S$, then the

following relation yields:

$$S_{conf}(T) \approx S_{conf}(0) + \int_0^T \frac{\Delta C_p}{T} dT. \quad (5)$$

Thus, in performing numerical integration of the area under DSC curve during a peak will produce a kink in S_{conf}, which in turn will produce a change in slope in the Angell plot of transport properties, as demonstrated elsewhere[47]. While there is uncertainty associated with the measured collective relaxation time quantified by both models, the resulting flattening in relaxation time between 950 – 1000 °C is consistently observed. Interestingly, a deviation of the self relaxation time from high temperature Arrhenius behavior, i.e. Arrhenius crossover or dynamical onset, has been observed around similar temperatures in both neutron scattering measurements and molecular dynamics simulations[48]. However, the link between the self and the fast collective relaxation times is not trivial in such metallic liquids. Furthermore, the Arrhenius crossover has not been found to correlate with a thermodynamic signature such as the heat capacity peak observed in this system. Hence, the coincidence of the collective relaxation anomaly and the specific heat peak indicates some interesting phenomenon happening at this temperature range that merits further study.

In a recent study, a similar peak in c_p of a Cu-Zr-Al based BMG has been attributed to an underlying temperature induced weak liquid-liquid phase transition characterized by change in length-scale of $S(Q)$[19]. The same interpretation has been applied to explain a similar non-monotonic nature of the measured viscosity[49]. Our result is consistent with, although do not corroborate, such interpretations. In general, a liquid-liquid phase transition is shown to exist if the interaction pair potential has two distinct length scales[50]. However, it is not known exactly how a liquid-liquid phase transition would manifest itself in a many-body interacted system. Another possible scenario for this behavior could be local structural separation in the liquid. Evidently, further experiments with with improved statistics are needed in order to elucidate the nature of the unusual change of slope in the collective relaxation times and its coincidence with the c_p peak beyond the melting point.

V. CONCLUSIONS

In summary, the QENS measurement of collective relaxations in a bulk-metallic glass-forming liquid (LM601 $Zr_{51}Cu_{36}Ni_4Al_9$) reveals an unusual change in slope of the temperature dependence of relaxation time around 950 °C for the kinetic Q range 1.5 – 4.0 Å^{-1}. This feature is independent of the models used for the data analysis. DSC measurements also reveal the presence of a peak in the same temperature range where the change of slope in relaxation times is observed. This coincidence may have interesting physical implications. Further QENS measurements with more temperature points and improved accuracy are required to understand the connection between observed unusual slope change of the collective relaxation time and the specific heat peak revealed in the DSC measurements.

ACKNOWLEDGMENTS

YZ is supported by NRC faculty development award NRC-HQ-12-G-38-0072 and UIUC Campus Research Board Award RB14187. YZ and TE are supported by the U.S. Department of Energy, Office of Sciences, Basic Energy Sciences, Materials Science and Engineering Division. Part of the Research conducted at ORNL's Spallation Neutron Source was sponsored by the Scientific User Facilities Division, Office of Basic Energy Sciences, US Department of Energy. We thank Prof. Brent Heuser and Peter Mouche at UIUC for their help with the DSC and TGA measurements using alumina cell, and Prof. James F. Stubbins and Kuan-Che Lan for help with cutting the samples using diamond saw.

[1] M. M. Trexler and N. N. Thadhani, Progress in Materials Science **55**, 759 (2010).
[2] M. F. Ashby and A. L. Greer, Scripta Materialia **54**, 321 (2006).
[3] J. Schroers and W. L. Johnson, Physical Review Letters **93**, 255506 (2004).
[4] J. F. Löffler, Intermetallics **11**, 529 (2003).
[5] Y. Wu, H. Wang, H. Wu, Z. Zhang, X. Hui, G. Chen, D. Ma, X. Wang, and Z. Lu, Acta Materialia **59**, 2928 (2011).
[6] A. L. Greer, Science **267**, 1947 (1995).
[7] A. I. Salimon, M. F. Ashby, Y. Bréchet, and A. L. Greer, Materials Science and Engineering A **375-377**, 385 (2004).
[8] A. Inoue and A. Takeuchi, Acta Materialia **59**, 2243 (2011).
[9] A. Inoue and W. Zhang, Materials Transactions **43**, 2921 (2002).
[10] Q. An, K. Samwer, W. A. Goddard, W. L. Johnson, A. Jaramillo-Botero, G. Garret, and M. D. Demetriou, The Journal of Physical Chemistry Letters **3**, 3143 (2012).
[11] W. L. Johnson, G. Kaltenboeck, M. D. Demetriou, J. P. Schramm, X. Liu, K. Samwer, C. P. Kim, and D. C. Hofmann, Science **332**, 828 (2011).
[12] A. Inoue, W. Zhang, T. Zhang, and K. Kurosaka, Acta Materialia **49**, 2645 (2001).
[13] D. Xu, G. Duan, and W. L. Johnson, Physical Review Letters **92**, 245504 (2004).
[14] Q. Jiang, X. Wang, X. Nie, G. Zhang, H. Ma, H.-J. Fecht, J. Bendnarcik, H. Franz, Y. Liu, Q. Cao, and J. Jiang, Acta Materialia **56**, 1785 (2008).

[15] W. Wang, C. Dong, and C. Shek, Materials Science and Engineering: R: Reports **44**, 45 (2004).
[16] M. Chen, NPG Asia Materials **3**, 82 (2011).
[17] N. A. Mauro, M. Blodgett, M. L. Johnson, A. J. Vogt, and K. F. Kelton, Nature Communications **5**, 1 (2014).
[18] T. Iwashita, D. M. Nicholson, and T. Egami, Physical Review Letters **110**, 205504 (2013).
[19] S. Wei, F. Yang, J. Bednarcik, I. Kaban, O. Shuleshova, A. Meyer, and R. Busch, Nature Communications **4**, 2083 (2013).
[20] T. Egami, Modern Physics Letters B **28**, 1430006 (2014).
[21] W. Götze, Condensed Matter Physics **1**, 873 (1998).
[22] W. Götze, Journal of Physics: Condensed Matter **11**, A1 (1999).
[23] W. Kob, in *Supercooled Liquids*, Vol. 676 (1997) pp. 28–44.
[24] D. R. Reichman and P. Charbonneau, Journal of Statistical Mechanics: Theory and Experiment **2005**, P05013 (2005).
[25] S. M. Chathoth, B. Damaschke, M. M. Koza, and K. Samwer, Physical Review Letters **101**, 037801 (2008).
[26] A. Meyer, J. Wuttke, W. Petry, O. G. Randl, and H. Schober, Physical Review Letters **80**, 4454 (1998).
[27] A. Meyer, J. Wuttke, and W. Petry, Journal of Non-Crystalline Solids **250**, 116 (1999).
[28] B. Kamgar-Parsi, E. G. D. Cohen, and I. M. de Schepper, Phys. Rev. A **35**, 4781 (1987).
[29] E. Cohen, I. D. Schepper, and M. Zuilhof, Physica B+C **127**, 282 (1984).
[30] T. Scopigno, G. Ruocco, and F. Sette, Reviews of Modern Physics **77**, 881 (2005).
[31] J.-P. Hansen and I. R. McDonald, *Theory of Simple Liquids*, 3rd ed. (Academic Press, 2006).
[32] A. Meyer, W. Petry, M. Koza, and M. P. Macht, Applied Physics Letters **83**, 3894 (2003).
[33] F. Yang, D. Holland-Moritz, J. Gegner, P. Heintzmann, F. Kargl, C. C. Yuan, G. G. Simeoni, and A. Meyer, Europhysics Letters **107**, 1 (2014).
[34] O. Arnold, J. C. Bilheux, J. M. Borreguero, A. Buts, S. I. Campbell, L. Chapon, M. Doucet, N. Draper, R. Ferraz Leal, M. A. Gigg, V. E. Lynch, A. Markvardsen, D. J. Mikkelson, R. L. Mikkelson, R. Miller, K. Palmen, P. Parker, G. Passos, T. G. Perring, P. F. Peterson, S. Ren, M. A. Reuter, A. T. Savici, J. W. Taylor, R. J. Taylor, R. Tolchenov, W. Zhou, and J. Zikovsky, Nuclear Instruments and Methods in Physics Research, Section A: Accelerators, Spectrometers, Detectors and Associated Equipment **764**, 156 (2014).
[35] R. T. Azuah, L. R. Kneller, Y. Qiu, P. L. W. Tregenna-Piggott, C. M. Brown, J. R. D. Copley, and R. M. Dimeo, Journal of Research of the National Institute of Standards and Technology **114**, 341 (2009).
[36] M. D. Ediger, Annual Review of Physical Chemistry **51**, 99 (2000).
[37] S. M. Chathoth and A. Podlesnyak, Journal of Applied Physics **103**, 013509 (2008).
[38] T. Kordel, D. Holland-Moritz, F. Yang, J. Peters, T. Unruh, T. Hansen, and A. Meyer, Physical Review B **83**, 104205 (2011).
[39] A. Meyer, Phys. Rev. B **66**, 134205 (2002).
[40] W. Gotze, Journal of Physics: Condensed Matter **2**, 8485 (1999).
[41] M. Fuchs, I. Hofacker, and A. Latz, Physical Review A **45**, 898 (1992).
[42] W. Petry and J. Wuttke, Transport Theory and Statistical Physics **24**, 1075 (1995).
[43] G. Li, W. M. Du, X. K. Chen, H. Z. Cummins, and N. J. Tao, Physical Review A **45**, 3867 (1992).
[44] E. Bartsch, F. Fujara, J. F. Legrand, W. Petry, H. Sillescu, and J. Wuttke, Physical Review E **52**, 738 (1995).
[45] W. van Megen and S. M. Underwood, Physical Review E **49**, 4206 (1994).
[46] G. Adam and J. H. Gibbs, The Journal of Chemical Physics **43**, 139 (1965).
[47] Y. Zhang, M. Lagi, D. Liu, F. Mallamace, E. Fratini, P. Baglioni, E. Mamontov, M. Hagen, and S.-H. H. Chen, The Journal of Chemical Physics **130**, 135101 (2009).
[48] A. Jaiswal, T. Egami, and Y. Zhang, Physical Review B **91**, 134204 (2015).
[49] C. Zhou, L. Hu, Q. Sun, J. Qin, X. Bian, and Y. Yue, Applied Physics Letters **103**, 171904 (2013).
[50] G. Franzese, G. Malescio, A. Skibinsky, S. V. Buldyrev, and H. E. Stanley, Nature **409**, 692 (2001).